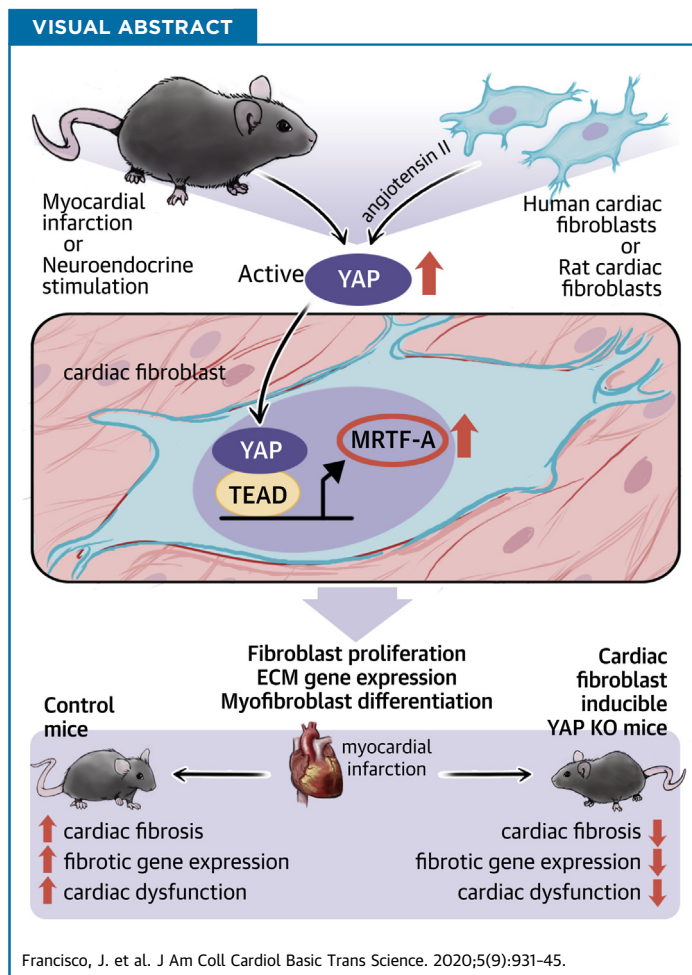


PRECLINICAL RESEARCH

# Blockade of Fibroblast YAP Attenuates Cardiac Fibrosis and Dysfunction Through MRTF-A Inhibition



Jamie Francisco, MS,<sup>a</sup> Yu Zhang, MS,<sup>a</sup> Jae Im Jeong, BS,<sup>a</sup> Wataru Mizushima, MD, PhD,<sup>a</sup> Shohei Ikeda, MD, PhD,<sup>a</sup> Andreas Ivessa, PhD,<sup>a</sup> Shinichi Oka, PhD,<sup>a</sup> Peiyong Zhai, MD, PhD,<sup>a</sup> Michelle D. Tallquist, PhD,<sup>b</sup> Dominic P. Del Re, PhD<sup>a</sup>



**HIGHLIGHTS**

- YAP is activated by myocardial infarction or neuroendocrine stimulation in cardiac fibroblasts.
- Active YAP promotes TEA domain transcription factor-1-mediated transcription of myocardin-related transcription factor A to facilitate cardiac myofibroblast differentiation and extra-cellular matrix gene expression.
- Cardiac fibroblast YAP knockout mice have attenuated cardiac fibrosis and dysfunction in response to myocardial infarction.

From the <sup>a</sup>Department of Cell Biology and Molecular Medicine, Cardiovascular Research Institute, Rutgers New Jersey Medical School, Newark, New Jersey; and the <sup>b</sup>Center for Cardiovascular Research, John A. Burns School of Medicine, University of Hawaii at Manoa, Honolulu, Hawaii. This study was supported by National Institutes of Health grants HL127339 and HL135726 (to Dr. Del Re). All other authors have reported that they have no relationships relevant to the contents of this paper to disclose. The authors attest they are in compliance with human studies committees and animal welfare regulations of the authors' institutions and Food and Drug Administration guidelines, including patient consent where appropriate. For more information, visit the *JACC: Basic to Translational Science* [author instructions page](#).

Manuscript received January 3, 2020; revised manuscript received July 27, 2020, accepted July 27, 2020.

## ABBREVIATIONS AND ACRONYMS

- AngII** = angiotensin II  
**MCM** = Mer-Cre-Mer  
**MI** = myocardial infarction  
**Mkl1** = megakaryoblastic leukemia 1  
**mRNA** = messenger ribonucleic acid  
**MRTF-A** = myocardin-related transcription factor A  
**NRCF** = neonatal rat cardiac fibroblast  
**PDGFR** = platelet-derived growth factor receptor  
**PE** = phenylephrine  
**SMA** = smooth muscle actin  
**TEAD** = TEA domain transcription factor  
**TGF** = transforming growth factor  
**YAP** = yes-associated protein

## SUMMARY

Fibrotic remodeling of the heart in response to injury contributes to heart failure, yet therapies to treat fibrosis remain elusive. Yes-associated protein (YAP) is activated in cardiac fibroblasts by myocardial infarction, and genetic inhibition of fibroblast YAP attenuates myocardial infarction-induced cardiac dysfunction and fibrosis. YAP promotes myofibroblast differentiation and associated extracellular matrix gene expression through engagement of TEA domain transcription factor 1 and subsequent de novo expression of myocardin-related transcription factor A. Thus, fibroblast YAP is a promising therapeutic target to prevent fibrotic remodeling and heart failure. (J Am Coll Cardiol Basic Trans Science 2020;5:931-45) © 2020 The Authors. Published by Elsevier on behalf of the American College of Cardiology Foundation. This is an open access article under the CC BY-NC-ND license (<http://creativecommons.org/licenses/by-nc-nd/4.0/>).

**F**ibrosis occurs in response to many types of cardiac injury, including myocardial infarction (MI), and is an important adaptive mechanism for preserving cardiac output in the face of massive cardiomyocyte loss (1). Pathological insults elicit activation of resident fibroblasts within the myocardium and promote their differentiation into myofibroblasts (2,3). This specialized cell type is characterized by robust secretion of extracellular matrix (ECM) proteins, as well as expression of  $\alpha$ -smooth muscle actin (SMA), which confers contractile function. These properties of myofibroblasts are critical to prevent wall rupture and promote wound healing in response to MI (4); however, prolonged fibrosis leads to excessive ECM deposition, remodeling, arrhythmia, impaired compliance, and ultimately heart failure (1). Therefore, a more complete understanding of the mechanisms underlying myofibroblast transition may facilitate the generation of effective therapeutic interventions for antagonizing this response.

Yes-associated protein (YAP) is the end effector of the Hippo pathway, an evolutionarily conserved signaling mechanism critical for the regulation of organ size (5). YAP responds to a variety of extracellular cues to enhance proliferation and survival in multiple cell and tissue types (6). Studies from our group and others have shown that activation of YAP in cardiomyocytes protects the heart against ischemic stress (7-10). Conversely, cardiomyocyte-restricted inhibition of YAP causes lethal dilated cardiomyopathy and predisposes mice to worsened cardiac remodeling and heart failure after MI (11,12). Importantly, nearly all cardiac studies involving YAP have focused on the cardiomyocyte, and YAP function in adult cardiac fibroblasts during myocardial injury remains largely unknown.

In the current paper, we determined the role of endogenous YAP in cardiac fibroblasts in the stressed

heart. Our findings show that YAP is activated in cardiac fibroblasts in response to nonreperfused MI, as well as angiotensin II (AngII) stimulation. Using fibroblast-restricted genetic inactivation of endogenous YAP, we show that YAP deletion attenuates myocardial fibrosis and cardiac dysfunction in response to MI or chronic neuroendocrine stimulation. Mechanistically, we report that YAP binds to the myocardin-related transcription factor A (MRTF-A) gene at putative TEA domain transcription factor (TEAD) recognition sites, and induces MRTF-A expression to facilitate myofibroblast transition and profibrotic gene expression.

## METHODS

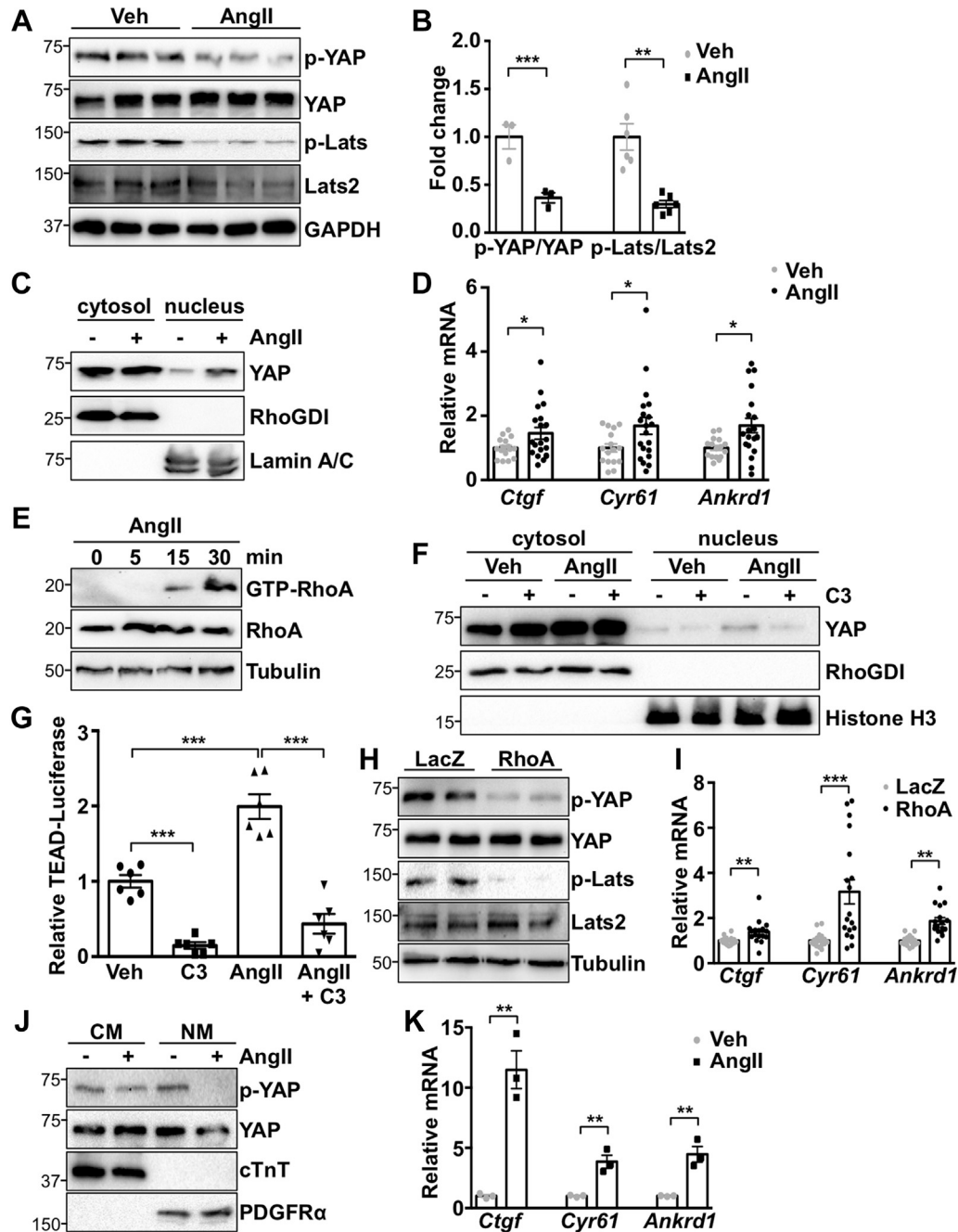
All methods and supporting data are available within the paper and the [Supplemental Methods and Supplemental Tables 1 and 2](#).

**ANIMAL MODELS.** Conditional *Yap1* allele floxed mice (13) were crossed with knockin mice containing Mer-Cre-Mer (MCM) inserted in the *Tcf21* locus (14) (*Yap<sup>F/F</sup>;Tcf21<sup>MCM</sup>*) or transgenic mice harboring tamoxifen-inducible CreERT2 driven by the *Col1a1* promoter (15) (*Yap<sup>F/F</sup>;Col1a1<sup>CreERT</sup>*) to generate conditional YAP-deleted mice. All mouse lines were C57BL/6J background. Age- and sex-matched littermate controls (*Yap<sup>F/F</sup>*) were used for all experiments, which were performed blinded to genotype.

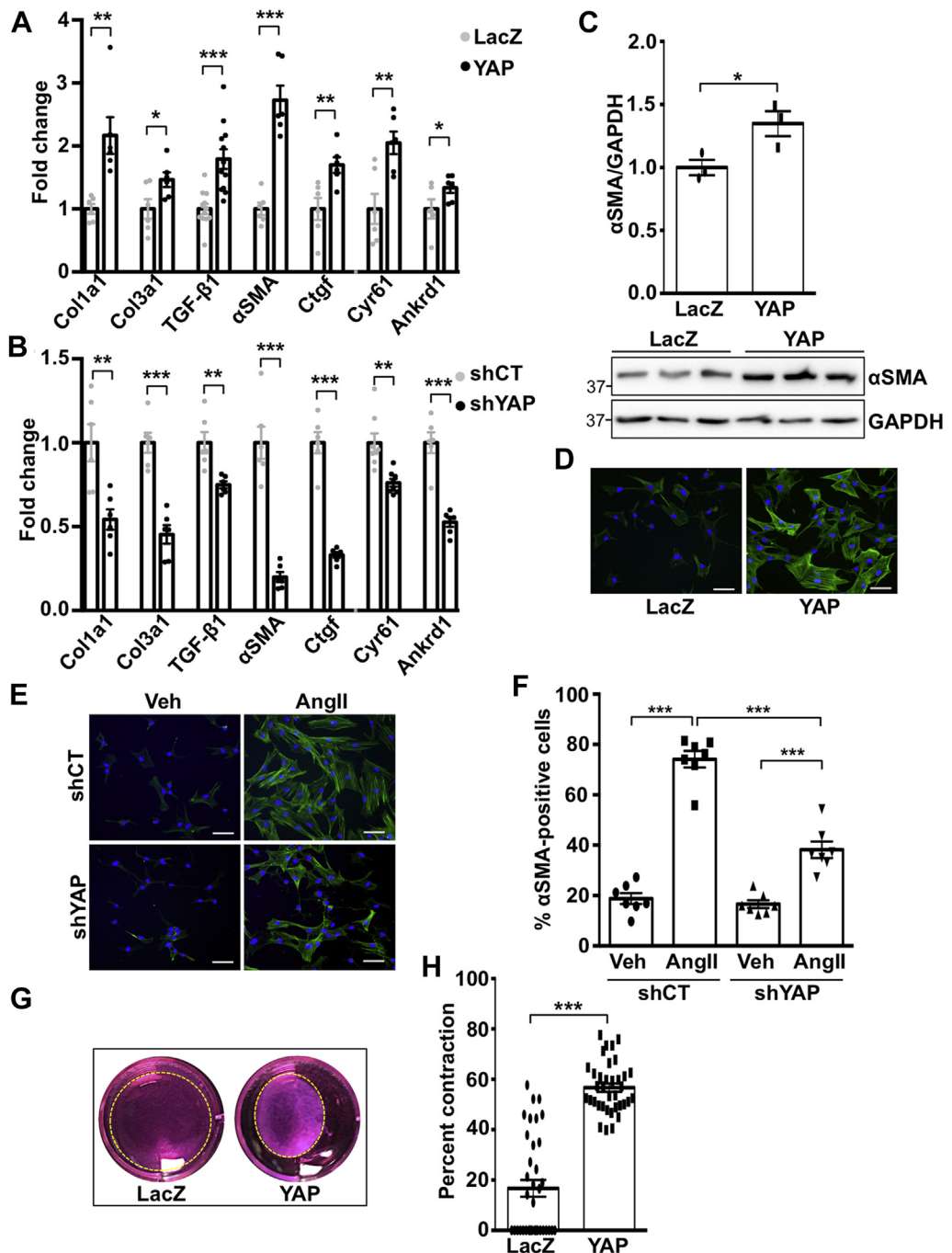
All protocols concerning the use of animals were approved by the Institutional Animal Care and Use Committee at Rutgers, The State University of New Jersey (New Brunswick, New Jersey).

**NONREPERFUSED MI.** Permanent left anterior descending coronary artery occlusion was used to induce MI, as previously described (11). Briefly, the left coronary artery was located, and a suture was passed under the artery. To occlude the artery, a short length of tubing was threaded through the suture ends, and occlusion was affected by placing tension

**FIGURE 1** AngII Activates YAP in Cardiac Fibroblasts

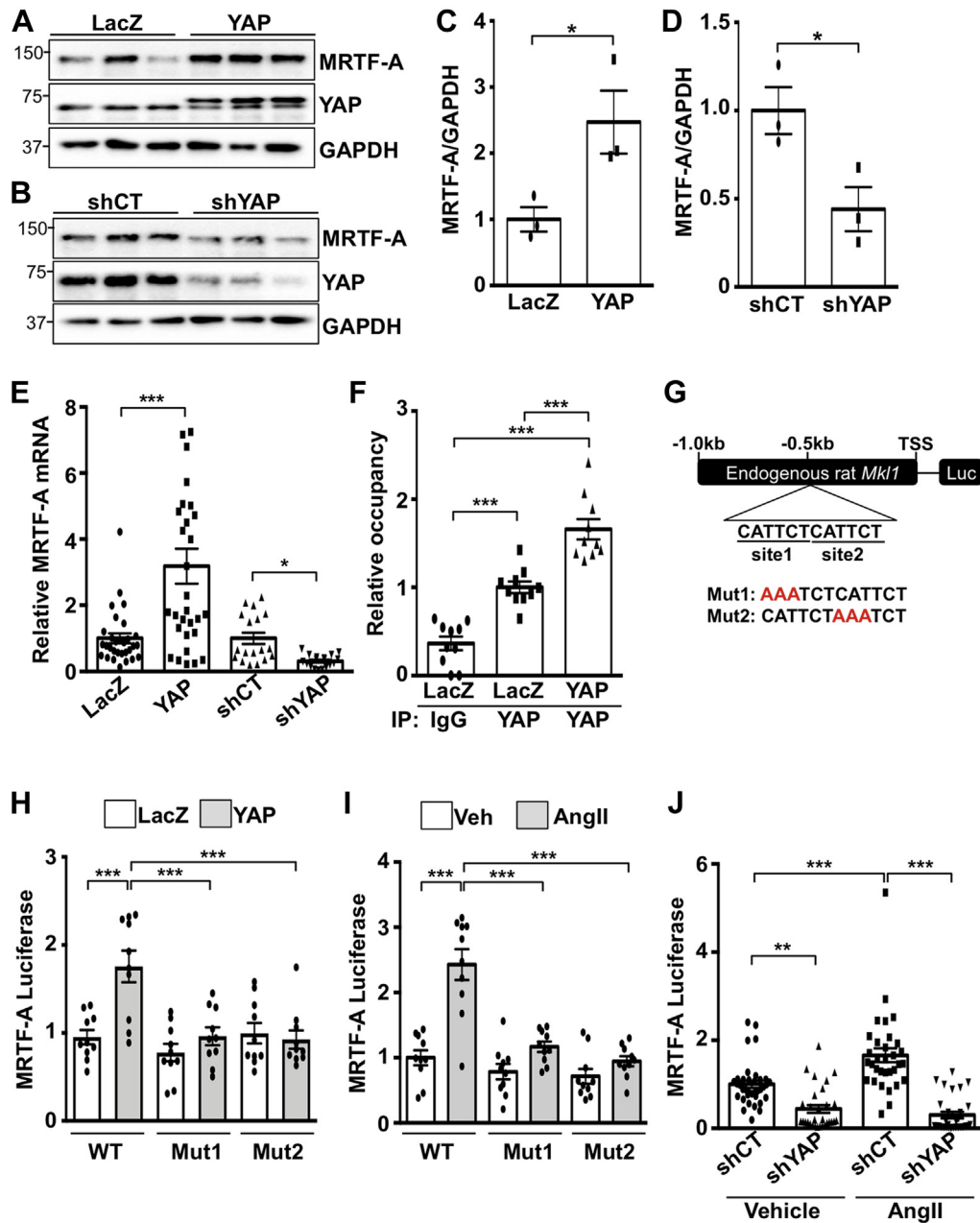


**(A to C)** Neonatal rat cardiac fibroblasts (NRCFs) were treated with angiotensin II (AngII) (100 nM) or vehicle (Veh) for 1 h, followed by subcellular fractionation and western blotting. **(D)** NRCFs were stimulated for 24 h, followed by quantitative polymerase chain reaction to detect Yes-associated protein (YAP) target genes. **(E)** RhoA was activated by AngII. **(F and G)** RhoA inhibitor pretreatment for 30 min (C3; 10 μM) prevented AngII-induced nuclear YAP and TEA domain transcription factor (TEAD) luciferase reporter activity. **(H and I)** RhoA expression activated YAP and increased YAP target genes. **(J and K)** Injection of AngII (1.0 μg/kg, intraperitoneally) activated YAP selectively in non-myocyte (NM) heart fractions from C57BL/6J mice after 1 h. Representative blots shown. N = 3 to 4 experiments. \*p < 0.05, \*\*p < 0.01, \*\*\*p < 0.001. Student's t-test was used for comparisons in all panels except panel G, where Tukey's post hoc test was used. ANKRD1 = Ankyrin repeat domain 1; CTGF = connective tissue growth factor; CYR61 = cysteine rich angiogenic inducer 61; cTnT = cardiac troponin T; GAPDH = glyceraldehyde-3-phosphate dehydrogenase; LacZ = β-galactosidase; Lats2 = large tumor suppressor kinase 2; mRNA = messenger ribonucleic acid; PDGFR = platelet-derived growth factor receptor.

**FIGURE 2** YAP Mediates Cardiac Myofibroblast Differentiation

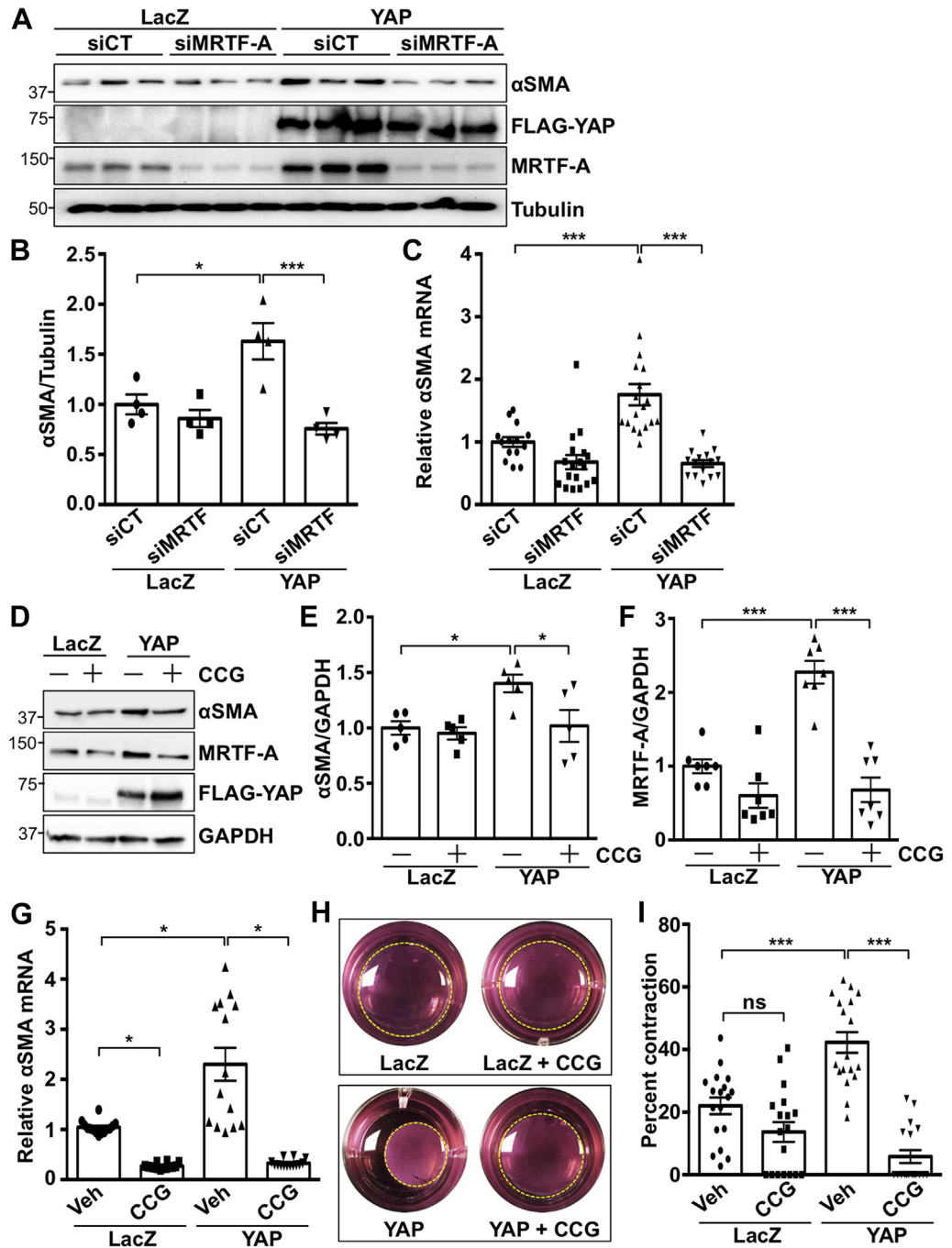
**(A and B)** Neonatal rat cardiac fibroblasts (NRCFs) were transduced with YAP or LacZ adenovirus for 24 h, or with short hairpin YAP (shYAP) or short hairpin control (shCT) adenovirus for 48 h, followed by quantitative polymerase chain reaction. **(C and D)** YAP expression increased  $\alpha$ -smooth muscle actin ( $\alpha$ SMA) protein. **(E and F)** YAP knockdown attenuated AngII-induced  $\alpha$ SMA-positive NRCFs. Percent positive cells were calculated based on 5 fields of view per well. **(G and H)** YAP expression in NRCFs increased collagen gel contraction. Representative blots shown.  $N = 3$  to 4 experiments. \* $p < 0.05$ , \*\* $p < 0.01$ , \*\*\* $p < 0.001$ . Student's t-test was used for comparisons in **all panels except panel F**, where Tukey's post hoc test was used. TGF = transforming growth factor; other abbreviations as in **Figure 1**.

**FIGURE 3** YAP Regulates the Transcription of MRTF-A in Cardiac Fibroblasts



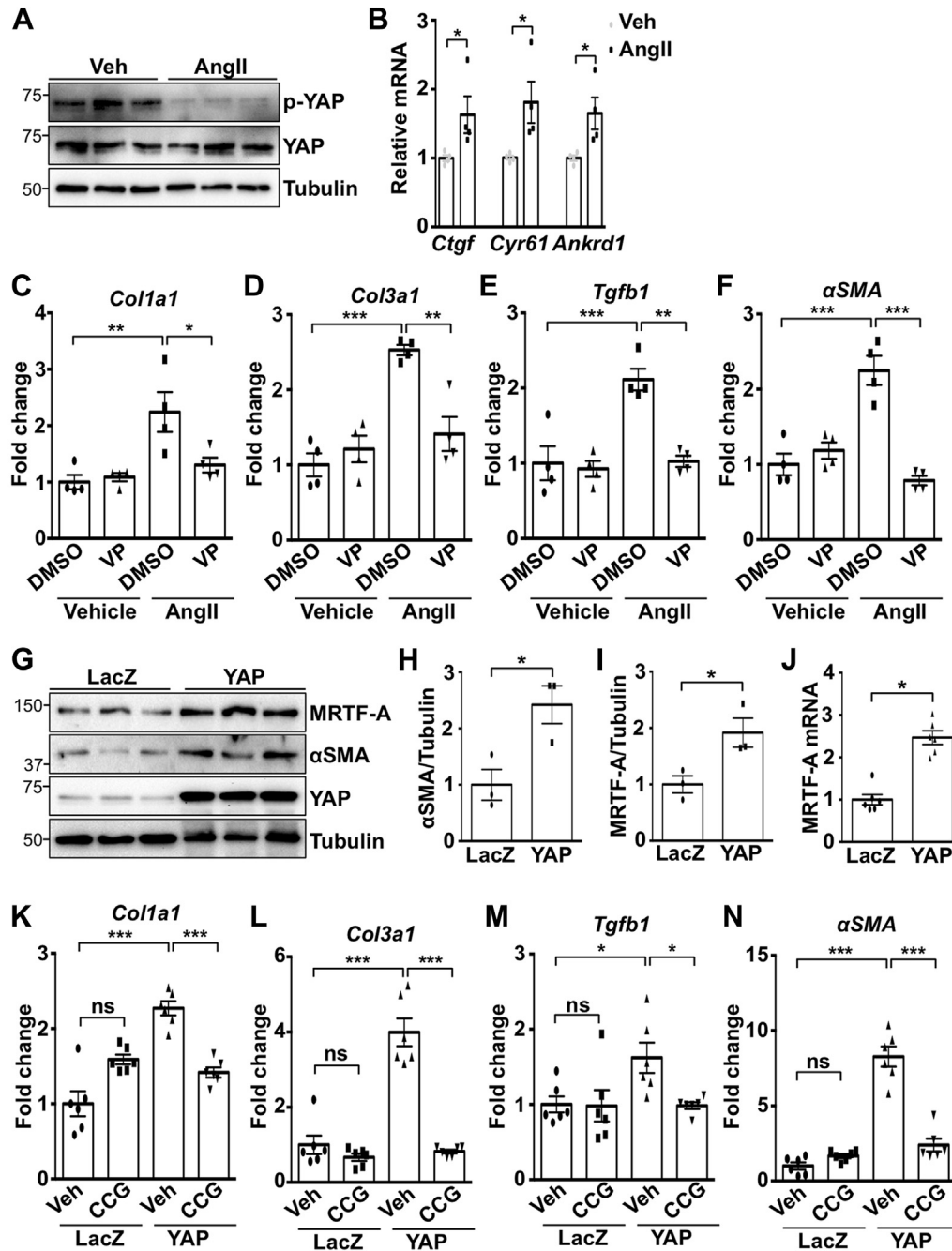
(A to E) NRCFs were transduced with YAP or LacZ adenovirus (24 h), or with shYAP or shCT (48 h), followed by western blot or quantitative polymerase chain reaction. (F) Chromatin immunoprecipitation assay to detect myocardin-related transcription factor A (MRTF-A) gene occupancy of YAP in NRCFs. (G) MRTF-A luciferase reporter construct consisting of the endogenous rat *Mkl1* gene sequence 1 kb proximal to the start of exon 1 (TSS). Tandem putative TEAD recognition motifs are highlighted. Two additional mutant constructs were generated by targeting TEAD binding site 1 (Mut1) or site 2 (Mut2) as shown in red. (H and I) YAP expression enhanced luciferase activity using the wild-type (WT) reporter construct but did not elicit significant activation of either mutant construct. Similar results were obtained by AngII treatment. (J) YAP knockdown prevented AngII-induced luciferase activity of the WT reporter construct in NRCFs. Representative blots shown. N = 3 to 4 experiments. \*p < 0.05, \*\*p < 0.01, \*\*\*p < 0.001. Student's t-test was used for comparisons in C to E. Tukey's post hoc test was used for comparisons in F and H to J. IgG = immunoglobulin G; other abbreviations as in Figures 1 and 2.

**FIGURE 4** MRTF-A Mediates YAP Induced Cardiac Myofibroblast Differentiation

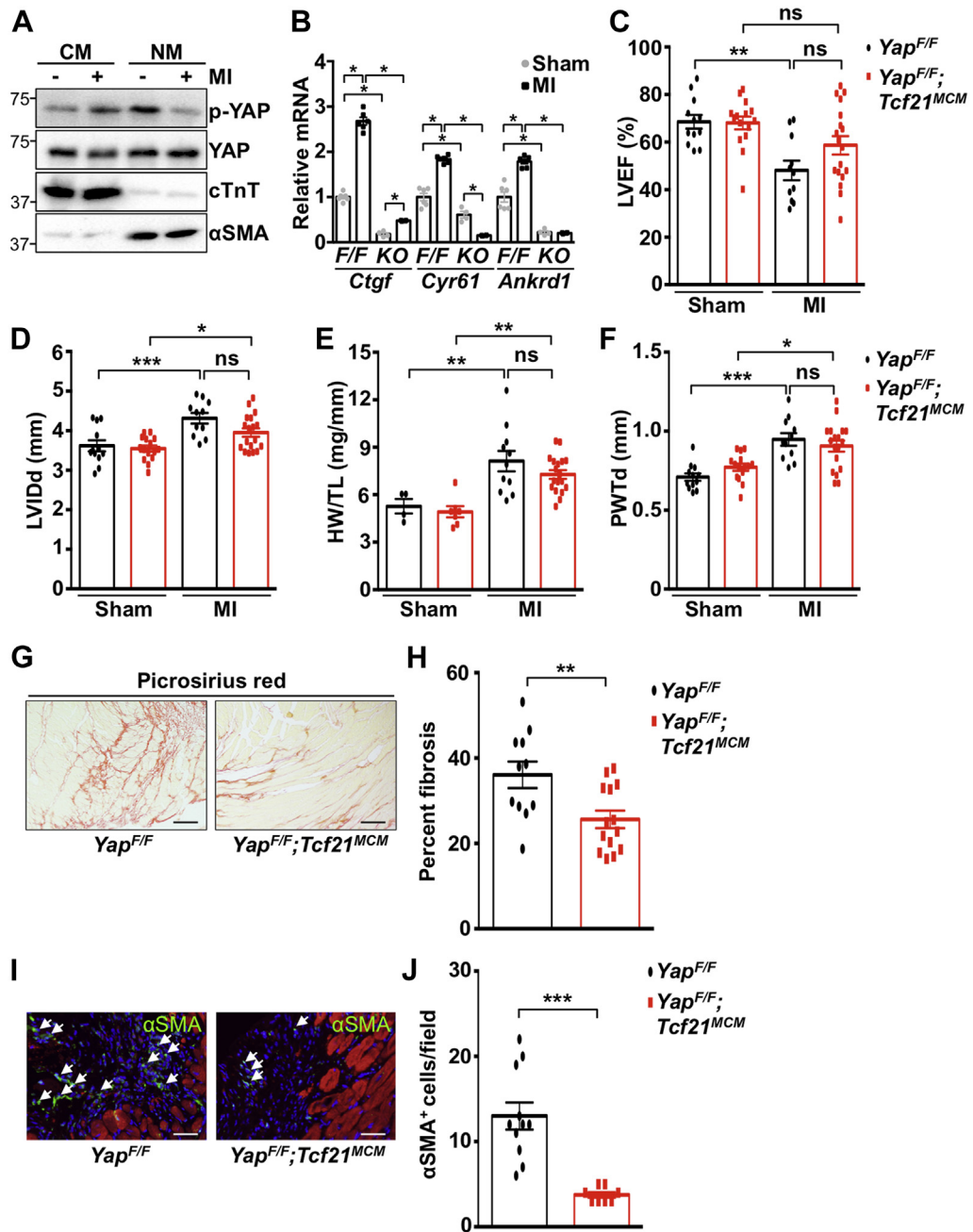


(A to C) MRTF-A knockdown prevented YAP-induced  $\alpha$ SMA expression in NRCFs. (D to G) The MRTF-A inhibitor CCG-203971 (CCG; 10  $\mu$ M) prevented YAP-induced  $\alpha$ SMA and MRTF-A expression in NRCFs. (H and I) MRTF-A inhibition prevented YAP-induced collagen gel contraction in NRCFs. Representative images shown. N = 3 to 4 experiments. \* $p$  < 0.05, \*\*\* $p$  < 0.001. ns = not significant. Tukey's post hoc test was used for all comparisons. siMRTF = short interfering MRTF-A RNA; siCT = short interfering control RNA; Other abbreviations as in Figures 1 to 3.

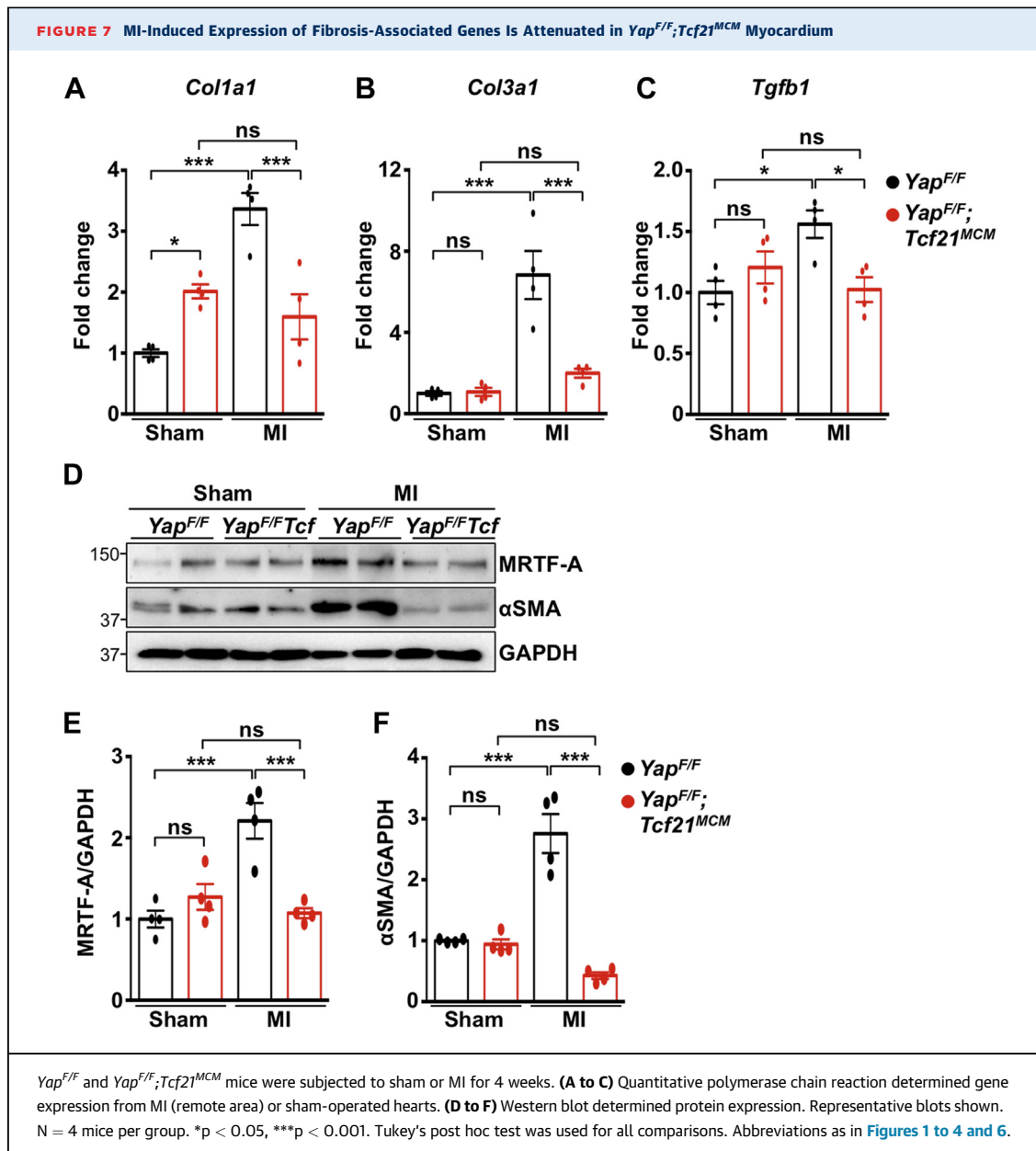
**FIGURE 5** YAP Promotes Human Cardiac Myfibroblast Differentiation Through Induction of MRTF-A



(**A and B**) Primary human ventricular fibroblasts were stimulated with AngII (100 nM) for 10 min and western blot performed, or for 24 h and YAP target genes determined by quantitative polymerase chain reaction. (**C to F**) Pretreatment for 30 min with the YAP inhibitor verteporfin (VP; 0.5 μM) prevented AngII-induced gene expression in human fibroblasts. (**G to J**) YAP expression increased MRTF-A and αSMA expression in human fibroblasts. (**K to N**) Pretreatment for 30 min with the MRTF-A inhibitor CCG-203971 (CCG; 10 μM) prevented YAP-induced gene expression in human fibroblasts. N = 3 to 4 experiments. \*p < 0.05, \*\*p < 0.01, \*\*\*p < 0.001. Student's t-test (**B, H to J**) and Tukey's post hoc test (**C to F and K to N**) were used for comparisons. DMSO = dimethyl sulfoxide; other abbreviations as in [Figures 1 to 4](#).

**FIGURE 6** Myocardial Fibrosis Is Attenuated in *Yap<sup>F/F</sup>;Tcf21<sup>MCM</sup>* Mice Following MI

(A) Three days after myocardial infarction (MI), WT C57BL/6J hearts were dissociated into cardiomyocyte- and NM-enriched fractions and used for western blotting. (B to J) *Yap<sup>F/F</sup>* and *Yap<sup>F/F</sup>;Tcf21<sup>MCM</sup>* mice were subjected to MI or sham. (B) NM-enriched fractions were used for quantitative polymerase chain reaction to detect YAP targets in mice of indicated genotypes (F/F = *Yap<sup>F/F</sup>*; KO = *Yap<sup>F/F</sup>;Tcf21<sup>MCM</sup>*). (C to F) Four weeks after MI, echocardiography and postmortem analysis were performed. (G and H) Fibrosis was attenuated in *Yap<sup>F/F</sup>;Tcf21<sup>MCM</sup>* post-MI hearts. Scale bar, 100  $\mu$ m. Representative images from remote region are shown. (I and J) Immunostaining was performed in post-MI hearts to detect  $\alpha$ SMA (green) and troponin-T (red). Arrows indicate  $\alpha$ SMA-positive NMs. Scale bar, 50  $\mu$ m. Representative images from infarct border region are shown. N = 4 to 18 mice/group. \* $p < 0.05$ , \*\* $p < 0.01$ , \*\*\* $p < 0.001$ . Student's t-test (H and J) and Tukey's post hoc test (B to F) were used for comparisons. LVEF = left ventricular ejection fraction; LVIDd = left ventricular end-diastolic dimension; PWTd = diastolic posterior wall thickness; HW/TL = heart weight to tibia length ratio other abbreviations as in Figures 1 to 5.



on the suture such that the tube compressed the artery. Ischemia was confirmed by electrocardiography change (ST-segment elevation). For sham operation, the same protocol was followed; however, no ligation of the coronary artery was performed.

**AngII/PHENYLEPHRINE TREATMENT.** Chronic AngII/phenylephrine (PE) infusion was attained by using osmotic mini-pumps (Alzet, Durect Corporation, Cupertino, California) that were implanted subcutaneously in 8- to 10-week-old mice under anesthesia (2.5% Avertin, 12  $\mu$ l/g body weight). AngII (288  $\mu$ g/kg/day) with PE (100 mg/kg/day) was delivered for 2 weeks as previously described (16). Control groups received vehicle infusion.

**CELL-BASED STUDIES.** Primary neonatal rat cardiac fibroblasts (NRCFs) and human ventricular fibroblasts were cultured as described elsewhere (7,17). Adenoviral transduction, transfection, luciferase reporter assays, chromatin immunoprecipitation, immunoblotting, immunostaining, quantitative polymerase chain reaction, and collagen gel contraction assays were performed using primary cells.

**STATISTICAL ANALYSIS.** All data are reported as mean  $\pm$  SEM. Evaluation between 3 or more groups was performed by using one-way analysis of variance. Post hoc multiple pairwise comparisons were performed by using Tukey's test. Student's t-test was used to evaluate the difference in means between 2

**TABLE 1 Echocardiographic Analysis of *Yap<sup>F/F</sup>;Tcf21<sup>MCM</sup>* Mice Subjected to MI**

	<i>Yap<sup>F/F</sup></i>		<i>Yap<sup>F/F</sup>;Tcf21<sup>MCM</sup></i>	
	Sham (n = 12)	MI (n = 11)	Sham (n = 15)	MI (n = 18)
LVIDd (mm)	3.57 ± 0.12	4.31 ± 0.13*	3.55 ± 0.09	3.95 ± 0.11†
LVIDs (mm)	2.23 ± 0.15	3.28 ± 0.19‡	2.22 ± 0.12	2.74 ± 0.16
IVSd (mm)	0.79 ± 0.03	0.79 ± 0.05	0.82 ± 0.02	0.88 ± 0.03
PWTd (mm)	0.71 ± 0.02	0.95 ± 0.04*	0.78 ± 0.02	0.91 ± 0.03†
LVEF (%)	68.6 ± 2.9	48.1 ± 4.1‡	68.1 ± 3.0	58.7 ± 3.9

Values are mean ± SEM. \*p < 0.001. †p < 0.05. ‡p < 0.01 versus respective sham.  
IVSd = diastolic septal wall thickness; LVEF = left ventricular ejection fraction; LVIDd = left ventricular end-diastolic dimension; LVIDs = left ventricular end-systolic dimension; MI = myocardial infarction; PWTd = diastolic posterior wall thickness.

groups. The normality of continuous variables was determined by using the Shapiro-Wilk test. Statistical analyses were performed by using GraphPad Prism version 8 (GraphPad Software, La Jolla, California). A p value < 0.05 was considered statistically significant.

## RESULTS

### YAP IS ACTIVATED BY AngII IN CARDIAC FIBROBLASTS.

To determine YAP activation in response to stress, primary NRCFs were stimulated with AngII. We observed a significant decrease in both YAP and large tumor suppressor kinase 2 (Lats) phosphorylation, indicating YAP activation (Figures 1A and 1B). AngII also increased YAP nuclear localization and YAP target gene expression in cardiac fibroblasts (Figures 1C and 1D). AngII treatment activated RhoA, and inhibition of RhoA with C3 toxin attenuated AngII-induced YAP nuclear localization and TEAD luciferase reporter gene activation (Figures 1E to 1G). In addition, expression of activated RhoA was sufficient to activate YAP (Figures 1H and 1I). Together, these data indicate that RhoA mediates AngII-stimulated YAP activation in cardiac fibroblasts.

To determine YAP activation status in vivo, we injected wild-type C57Bl/6J mice with AngII, isolated hearts after 1 h, and generated cardiomyocyte and nonmyocyte-enriched fractions. Fraction purity was determined by expression of cardiomyocyte-specific and fibroblast-specific markers, troponin T, and

platelet-derived growth factor receptor (PDGFR)- $\alpha$ , respectively. AngII treatment increased YAP activation, as determined by phosphorylation, as well as YAP target gene expression, in fibroblast-enriched fractions, indicating that AngII activates YAP in vivo (Figures 1J and 1K).

### YAP MEDIATES AngII-INDUCED MYOFIBROBLAST DIFFERENTIATION.

AngII drives myofibroblast transition, which contributes to fibrotic remodeling in the heart (1). To investigate if YAP mediates this process, we first determined expression of established profibrotic genes in fibroblasts subjected to increased or decreased YAP expression. YAP expression significantly up-regulated *Col1a1*, *Tgf $\beta$ 1*, and  $\alpha$ SMA messenger ribonucleic acid (mRNA), as well as the established YAP target genes *Ctgf*, *Cyr61*, and *Ankrd1*. Conversely, knockdown of endogenous YAP significantly down-regulated these genes (Figures 2A and 2B). Increased de novo expression of  $\alpha$ -SMA is a marker of the myofibroblast phenotype. YAP expression caused a significant increase in  $\alpha$ -SMA protein levels (Figures 2C and 2D). Our data also show that  $\alpha$ SMA-positive cardiac fibroblasts were increased by AngII treatment, and this outcome was significantly attenuated in YAP-depleted cells (Figures 2E and 2F). We also assayed the ability of fibroblasts to contract a collagen lattice in response to YAP overexpression and found it was significantly enhanced (Figures 2G and 2H). Using overexpression and knockdown approaches, we show that YAP increases cardiac fibroblast proliferation, as determined by Ki-67, phosphorylated histone H3, and cell viability assay, indicating functional consequences of YAP activation in the cardiac fibroblast (Supplemental Figure 1).

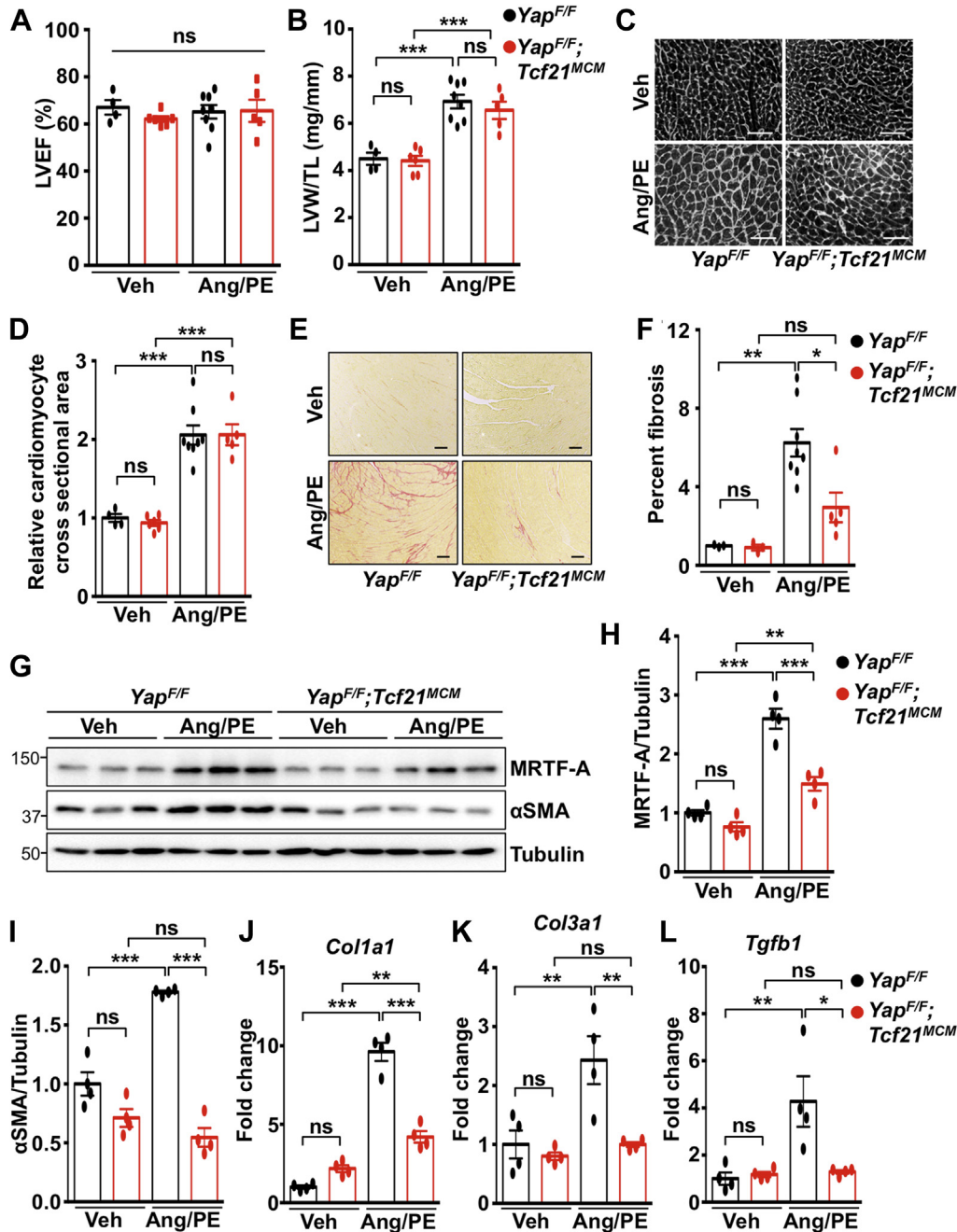
**YAP PROMOTES MRTF-A EXPRESSION.** To elucidate how YAP regulates myofibroblast differentiation, we investigated the role of MRTF-A, a transcriptional coactivator that mediates pro-fibrotic gene expression in the heart (18). Prior research indicates transcriptional cooperation between YAP and MRTF-A (19); however, very little is known regarding the regulation of MRTF-A expression itself. We found that increased YAP up-regulated MRTF-A mRNA and protein in cardiac fibroblasts. Conversely, knockdown of YAP decreased MRTF-A protein and mRNA (Figures 3A to 3E), indicating that YAP positively regulates MRTF-A through enhanced transcription. Examination of the rat *Mkl1* (MRTF-A) gene revealed 2 putative TEAD consensus-binding sequences ~500 bp upstream of the start of exon 1. In mouse and human *Mkl1*, we identified 1 conserved TEAD motif located at approximately the same position proximal to exon 1, as well as a second site ~600 bp further upstream, indicating a certain degree of conservation between species.

**TABLE 2 Echocardiographic Analysis of *Yap<sup>F/F</sup>;Col1a1<sup>CreERT</sup>* Mice Subjected to MI**

	<i>Yap<sup>F/F</sup></i>		<i>Yap<sup>F/F</sup>;Col1a1<sup>CreERT</sup></i>	
	Sham (n = 8)	MI (n = 10)	Sham (n = 7)	MI (n = 15)
LVIDd (mm)	3.49 ± 0.15	4.48 ± 0.24*	3.61 ± 0.11	4.23 ± 0.14†
LVIDs (mm)	1.98 ± 0.20	3.59 ± 0.29‡	2.43 ± 0.19	2.93 ± 0.17§
IVSd (mm)	0.86 ± 0.02	0.78 ± 0.05	0.88 ± 0.04	0.91 ± 0.04
PWTd (mm)	0.83 ± 0.03	0.97 ± 0.05	0.79 ± 0.04	1.00 ± 0.03*
LVEF (%)	74.7 ± 3.7	41.9 ± 5.0‡	66.9 ± 4.3	57.5 ± 2.9§

Values are mean ± SEM. \*p < 0.01. †p < 0.05. ‡p < 0.001 versus respective sham. §p < 0.05. ||p < 0.01 versus *Yap<sup>F/F</sup>* MI.  
Abbreviations as in Table 1.

**FIGURE 8** Fibrosis Is Attenuated in *Yap<sup>F/F</sup>;Tcf21<sup>MCM</sup>* Hearts Following Chronic AngII With PE Infusion



*Yap<sup>F/F</sup>* and *Yap<sup>F/F</sup>;Tcf21<sup>MCM</sup>* mice were subjected to continuous infusion of AngII (288  $\mu$ g/kg per day) with phenylephrine (PE) (100 mg/kg per day) or Veh control using osmotic mini-pumps. **(A)** Cardiac function (LVEF) was determined after a 2-week infusion. **(B to F)** After 2 weeks, postmortem and histological analyses were performed. **(C and D)** Cardiomyocyte area was determined by wheat germ agglutinin (WGA) staining. Scale bar, 100  $\mu$ m. **(E and F)** Fibrosis was attenuated in *Yap<sup>F/F</sup>;Tcf21<sup>MCM</sup>* hearts post-infusion. Scale bar, 100  $\mu$ m. **(G to I)** Western blotting and **(J to L)** quantitative polymerase chain reaction were performed using left ventricular tissue. N = 4 to 8 mice per group. \* $p < 0.05$ , \*\* $p < 0.01$ , \*\*\* $p < 0.001$ . Tukey's post hoc test was used for all comparisons. Abbreviations as in **Figures 4, 6, and 7**.

We performed chromatin immunoprecipitation in NRCFs using anti-YAP antibody and observed enrichment of YAP at this predicted TEAD-binding site (Figure 3F), indicating MRTF-A gene occupancy. Luciferase assays were performed by using the endogenous 1 kb region proximal to exon 1 of the rat *Mkl1* gene to drive reporter gene expression (Figure 3G). We tested the wild-type sequence, as well as 2 different mutant constructs that were generated by targeting TEAD-binding sites 1 and 2. Overexpression of YAP was sufficient to enhance luciferase expression using the wild-type construct; however, YAP-induced reporter gene expression was prevented in both mutant constructs (Figure 3H). Similar results were obtained with AngII treatment, indicating that both sites are necessary for reporter gene induction (Figure 3I). In addition, YAP knockdown abolished AngII-induced luciferase activation of the wild-type construct in cardiac fibroblasts (Figure 3J). Treatment of NRCFs with verteporfin, an inhibitor that prevents YAP-TEAD association, decreased baseline MRTF-A and  $\alpha$ SMA expression, and attenuated AngII-induced up-regulation of MRTF-A and  $\alpha$ SMA protein (Supplemental Figure 2). Similarly, knockdown of endogenous TEAD1 abolished YAP-induced increases in MRTF-A and  $\alpha$ SMA protein (Supplemental Figure 3). These results show that endogenous YAP occupies the MRTF-A gene and functions with TEAD1 to regulate MRTF-A expression.

**MRTF-A MEDIATES YAP STIMULATION OF MYOFIBROBLAST DIFFERENTIATION.** We next investigated the functional importance of MRTF-A as a downstream target of YAP. After MRTF-A depletion, YAP-induced  $\alpha$ SMA mRNA and protein expression were significantly attenuated (Figures 4A to 4C), implicating MRTF-A as a critical mediator of pro-fibrotic gene expression elicited by YAP. We also tested whether the MRTF-A inhibitor CCG-203971 (20) could influence YAP-induced signaling and functional effects in cardiac fibroblasts. The results show that CCG-203971 treatment significantly attenuated YAP-induced increases in  $\alpha$ -SMA mRNA and protein, as well as collagen lattice contraction (Figures 4D to 4I). These data indicate a fundamental role for MRTF-A in YAP-mediated responses.

**YAP FUNCTION IN HUMAN CARDIAC MYOFIBROBLAST DIFFERENTIATION.** Importantly, we determined YAP function in primary adult human ventricular fibroblasts. Our findings show that AngII activated YAP in human cardiac fibroblasts (Figures 5A and 5B). Treatment with AngII also up-regulated mRNA expression of *Col1a1*, *Col3a1*, *Tgfb1*, and  *$\alpha$ SMA*, which was prevented by verteporfin, indicating YAP-TEAD dependence (Figures 5C to 5F). YAP expression was

sufficient to increase pro-fibrotic gene expression, as well as MRTF-A and  $\alpha$ -SMA mRNA and protein in human cardiac fibroblasts (Figures 5G to 5J). In addition, this response was attenuated by CCG-203971, indicating that MRTF-A is an important target of YAP to mediate myofibroblast differentiation in human cardiac cells (Figures 5K to 5N).

**INHIBITORY TARGETING OF FIBROBLAST YAP IN VIVO ATTENUATES FIBROSIS AFTER MI.** We next investigated how loss of fibroblast YAP expression affected collagen deposition in the heart after injury. We found that YAP was activated in fibroblast-enriched heart fractions after 3 days of non-reperfusion MI (Figures 6A and 6B). To investigate YAP function in vivo, we generated mice lacking YAP in fibroblasts using 2 different tamoxifen-inducible Cre recombinase mouse lines. *Tcf21<sup>MCM</sup>* was used to delete YAP in quiescent cardiac fibroblasts (14) (*Yap<sup>F/F</sup>;Tcf21<sup>MCM</sup>*), and no baseline cardiac phenotype was observed (Table 1) despite decreased YAP protein in fibroblast-enriched heart fractions (Supplemental Figure 4). We then subjected mice to MI by permanent left anterior descending coronary artery occlusion. No difference was observed in initial injury between genotypes 1 day after ligation (Supplemental Figure 5). Similarly, no incidence of cardiac rupture was observed, and no significant difference in survival occurred between groups after MI (Supplemental Figure 6). In floxed control mice, cardiac function (left ventricular ejection fraction) was significantly decreased 4 weeks after MI compared with sham; however, function was preserved in *Yap<sup>F/F</sup>;Tcf21<sup>MCM</sup>* mice after MI (Figure 6C). Cardiac diastolic chamber and wall dimensions, as well as cardiac hypertrophy, were similar between control mice and *Yap<sup>F/F</sup>;Tcf21<sup>MCM</sup>* mice at baseline and after MI (Figures 6D to 6F, Supplemental Figure 7). However, a significant reduction in remote area terminal deoxynucleotidyl transferase dUTP nick end labeling-positive cardiomyocyte nuclei was observed in *Yap<sup>F/F</sup>;Tcf21<sup>MCM</sup>* mice compared with control mice.

Importantly, we also assessed the extent of fibrosis after MI. Although scar size trended smaller in *Yap<sup>F/F</sup>;Tcf21<sup>MCM</sup>* hearts, statistical significance was not attained (Supplemental Figure 8); however, *Yap<sup>F/F</sup>;Tcf21<sup>MCM</sup>* mice exhibited significant attenuation of collagen deposition throughout the left ventricle, as determined by Picrosirius red staining (Figures 6G and 6H). We also observed fewer cycling fibroblasts (Ki-67<sup>+</sup>PDGFR- $\alpha$ <sup>+</sup> cells), indicating less proliferation, and fewer fibroblasts overall (PDGFR- $\alpha$ <sup>+</sup> cells) in the infarct and border regions of *Yap<sup>F/F</sup>;Tcf21<sup>MCM</sup>* hearts 3 days after MI (Supplemental Figure 9). In addition, the number of  $\alpha$ SMA-positive

cells in the infarct and border zone of *Yap<sup>F/F</sup>;Tcf21<sup>MCM</sup>* mice was attenuated compared with control mice, indicating the reduced presence of myofibroblasts in *Yap<sup>F/F</sup>;Tcf21<sup>MCM</sup>* hearts after MI (Figures 6I and 6J). Analyses using *Col1a1<sup>CreERT</sup>* (*Yap<sup>F/F</sup>;Col1a1<sup>CreERT</sup>*) to remove YAP expression in cardiac fibroblasts (21) yielded similar results to those observed in *Yap<sup>F/F</sup>;Tcf21<sup>MCM</sup>* mice (Table 2, Supplemental Figures 4, 6, 8 to 13). Determination of ECM-related gene expression in the remote area revealed attenuated *Col1a1*, *Col3a1*, and *Tgfb1* mRNA in *Yap<sup>F/F</sup>;Tcf21<sup>MCM</sup>* hearts after MI compared with control mice (Figures 7A to 7C). Protein expression of MRTF-A and  $\alpha$ SMA was also attenuated in *Yap<sup>F/F</sup>;Tcf21<sup>MCM</sup>* mice after MI (Figures 7D to 7F). Together, these results indicate that depletion of fibroblast YAP prevents MRTF-A induction, attenuates fibroblast proliferation, and impedes myofibroblast transition, collagen deposition, and cardiac dysfunction that develop in response to nonreperfused MI in mice.

**YAP DELETION IN FIBROBLASTS ATTENUATES FIBROSIS CAUSED BY NEUROENDOCRINE STIMULATION.** We also modeled chronic injury to drive cardiac hypertrophy and fibrosis by continuous infusion of AngII with PE as previously described (16). No difference in cardiac function or hypertrophy was observed between control mice and YAP-deficient mice infused with AngII/PE for 2 weeks (Figures 8A to 8D, Table 3). However, fibrosis was significantly attenuated in *Yap<sup>F/F</sup>;Tcf21<sup>MCM</sup>* hearts compared with control hearts (Figures 8E and 8F). Protein analysis revealed significant attenuation of MRTF-A and  $\alpha$ SMA in left ventricular tissue isolated from *Yap<sup>F/F</sup>;Tcf21<sup>MCM</sup>* mice compared with *Yap<sup>F/F</sup>* mice after AngII/PE treatment (Figures 8G to 8I). Attenuation of *Col1a1*, *Col3a1*, and *Tgfb1* mRNA in *Yap<sup>F/F</sup>;Tcf21<sup>MCM</sup>* hearts was also observed (Figures 8J to 8L). Taken together, these results show that fibroblast YAP is a critical factor that necessitates adverse fibrosis in the heart in response to clinically relevant disease stimuli.

## DISCUSSION

The current study examined the function of endogenous YAP in cardiac fibroblasts. We observed YAP activation in fibroblast-enriched heart fractions in response to both nonreperfused MI and AngII stimulation in vivo, suggesting that multiple types of stress are competent to stimulate YAP in this cellular compartment. Importantly, deletion of fibroblast YAP significantly attenuated cardiac fibrosis and prevented cardiac dysfunction after MI or chronic neuroendocrine stimulation. In addition, the ability of YAP to mediate myofibroblast differentiation seems conserved to human cardiac fibroblasts.

**TABLE 3 Echocardiographic Analysis of *Yap<sup>F/F</sup>;Tcf21<sup>MCM</sup>* Mice Subjected to AngII/PE Infusion**

	<i>Yap<sup>F/F</sup></i>		<i>Yap<sup>F/F</sup>;Tcf21<sup>MCM</sup></i>	
	Vehicle (n = 4)	AngII/PE (n = 8)	Vehicle (n = 6)	AngII/PE (n = 5)
LVIDd (mm)	3.65 ± 0.26	3.49 ± 0.10	3.94 ± 0.10	3.15 ± 0.10*
LVIDs (mm)	2.33 ± 0.24	2.28 ± 0.13	2.64 ± 0.09	2.05 ± 0.15
IVSd (mm)	0.79 ± 0.06	0.86 ± 0.05	0.73 ± 0.04	0.86 ± 0.04
PWTd (mm)	0.65 ± 0.05	0.81 ± 0.04	0.72 ± 0.05	0.83 ± 0.03
LVEF (%)	67.0 ± 3.1	65.1 ± 2.7	62.1 ± 1.2	65.6 ± 4.3

Values are mean ± SEM. \*p < 0.05 versus respective vehicle.  
 AngII = angiotensin II; PE = phenylephrine; other abbreviations as in Table 1.

Together, these results show a pathological role for fibroblast YAP in adverse cardiac remodeling and suggest that YAP may represent a novel therapeutic target for the treatment of fibrosis and heart failure.

Studies regarding YAP function in lung (22), liver (23), and kidney (24) fibroblasts have reported positive effects on proliferative, contractile, and migratory capacity. Genetic inhibition of the Hippo pathway in cardiac fibroblasts via *Lats1/2* deletion elicited a pro-fibrotic response, which was exacerbated by MI and largely attenuated by concomitant suppression of YAP/transcriptional coactivator with PDZ-binding motif (TAZ), suggesting that endogenous inhibition of YAP/TAZ via Hippo restrains cardiac fibrosis (25). This is consistent with our current findings. We observed that fibroblast YAP activation is limited at baseline, and deletion of YAP in fibroblasts in the absence of injury has no obvious cardiac effect. In addition, we found a salutary effect of fibroblast YAP inhibition during MI, similar to previous observations. Interestingly, heightened fibroblast YAP/TAZ activity in the *Lats1/2*-deficient mice augmented non-cell autonomous apoptosis, an effect consistent with our observation of reduced cardiomyocyte apoptosis in fibroblast YAP-deficient mice post-MI. Taken together, our findings are predominantly in accord with other reports, yet advance the field by: 1) demonstrating endogenous YAP activation in heart fibroblast fractions after ischemic or neuroendocrine stress; 2) elucidating a pathological role of fibroblast YAP in cardiac fibrosis and dysfunction; 3) demonstrating that pharmacological inhibition of YAP-TEAD prevents cardiac myofibroblast activation; and 4) providing a novel mechanistic layer of MRTF-A regulation that underlies YAP function.

Several established signaling pathways that modulate cardiac fibrosis have been defined, including transforming growth factor (TGF)- $\beta$ -Smads, p38 $\alpha$ , transient receptor potential cation channel subfamily C member 6 (TRPC6)-calcineurin-nuclear factor of activated T cells (NFAT), and RhoA-MRTF-serum

response factor (SRF) (16,18,26-28). Although the functional importance of each has been documented in isolation, there is also convincing evidence of interpathway communication leading to complex signaling networks that modulate fibrosis (28). RhoA signaling directs the nuclear localization of MRTF-A to control ECM-related genes (29-31), and the Hippo-YAP pathway intersects with MRTF-A and SRF to further modulate gene expression (19,32). However, the regulation of MRTF-A expression itself is largely unexplored. To our knowledge, investigation of transcriptional regulation of MRTF-A in models of heart failure has not been reported, although AngII and PE stimulation have been shown to up-regulate MRTF-A expression in neonatal rat cardiomyocytes (33). Mechanistically, we show that YAP associates at 2 putative TEAD-response elements in the *Mkl1* gene and promotes the transcription and expression of MRTF-A in cardiac fibroblasts. Previous reports have linked YAP to TGF- $\beta$ -Smad and RhoA signaling (19,32,34). In the current study, we observed YAP-mediated regulation of TGF- $\beta$ 1 expression in cardiac fibroblasts, indicating the potential for cross-talk between these pathways, and it will be of interest to determine whether YAP influences TGF- $\beta$ -Smad signaling to further modulate cardiac fibrosis. We also found that AngII-induced activation of YAP is mediated by RhoA, indicating that RhoA likely serves as a nodal point to integrate regulatory signals during myofibroblast differentiation (35).

Previous research showed that MRTF-A null mice have smaller left ventricular scars, less fibrosis, and attenuated ECM gene expression after MI (18). Our results in fibroblast YAP-deficient mice showed similar effects on fibrosis and heart function. We predict this is a result of limiting the proliferative capacity of cardiac fibroblasts and myofibroblast differentiation mediated by YAP; however, we cannot rule out additional mechanisms, including potential paracrine effects on other cell types such as cardiomyocytes, macrophages, and vascular cells. Indeed, we observed reduced cardiomyocyte apoptosis in fibroblast YAP-deficient hearts. The protection resulting from fibroblast YAP targeting is a striking contrast to the effect of cardiomyocyte-specific YAP deletion, which causes worsened cardiac remodeling and function after MI (11,12) and reinforces the importance of cell type specificity of signaling in the heart.

The current study reports a relatively mild MI as determined by left ventricular functional decline, chamber dilation, and scar size. Although we determined the initial infarct, and found no differences between control mice and YAP-targeted mice (Supplemental Figure 5), it is difficult to directly

compare extent of injury/area at risk versus previous reports as most studies do not include these data (36). Based on our results, fibroblast deletion of YAP provides benefit for ischemia-induced remodeling and does not alter the likelihood of cardiac rupture or death after MI (Supplemental Figure 6). However, this does not preclude the possibility that YAP may also have a reparative function post-MI, which might be apparent in the context of a larger infarct.

**STUDY LIMITATIONS.** We conducted this investigation in male mice. Sex differences in MI injury have been reported (37). Verteporfin has been shown to effectively inhibit YAP-TEAD function in vivo; however, studies using TEAD1-deficient mice to rule out potential off-target effects would be ideal.

## CONCLUSIONS

Our findings identified a YAP-MRTF-A signaling axis in cardiac fibroblasts and show a fundamental role for YAP in modulating the myofibroblast phenotype and cardiac fibrosis in response to injury. We describe an opposing and detrimental function of YAP in cardiac fibroblasts compared with the protective function of YAP in cardiomyocytes. This work underscores the impact of selective YAP targeting on heart remodeling and dysfunction during chronic stress, and raises the potential of therapeutic targeting of fibroblast YAP for translational applications.

**ACKNOWLEDGMENT** The authors thank Junichi Sadoshima (Rutgers New Jersey Medical School) for valuable insight and discussion.

**ADDRESS FOR CORRESPONDENCE:** Dr. Dominic P. Del Re, Rutgers New Jersey Medical School, 185 South Orange Avenue, MSB G-609, Newark, New Jersey 07103. E-mail: [delredo@njms.rutgers.edu](mailto:delredo@njms.rutgers.edu).

## PERSPECTIVES

### COMPETENCY IN MEDICAL KNOWLEDGE:

Fibrosis is one of the major components of adverse cardiac remodeling and the transition to heart failure. Inhibition of YAP activity in cardiac fibroblasts attenuates post-infarction fibrosis and ventricular dysfunction in mice by limiting myofibroblast differentiation, proliferation, and ECM production.

**TRANSLATIONAL OUTLOOK:** Future studies are warranted to determine the potential therapeutic benefit of YAP inhibition in cardiac fibroblasts for the prevention of cardiac remodeling and heart failure following infarction.

## REFERENCES

1. Prabhu SD, Frangogiannis NG. The biological basis for cardiac repair after myocardial infarction: from inflammation to fibrosis. *Circ Res* 2016;119:91-112.
2. Kanisicak O, Khalil H, Ivey MJ, et al. Genetic lineage tracing defines myofibroblast origin and function in the injured heart. *Nat Commun* 2016;7:12260.
3. Ivey MJ, Kuwabara JT, Pai JT, Moore RE, Sun Z, Tallquist MD. Resident fibroblast expansion during cardiac growth and remodeling. *J Molec Cellular Cardiol* 2018;114:161-74.
4. Shimazaki M, Nakamura K, Kii I, et al. Periostin is essential for cardiac healing after acute myocardial infarction. *J Exp Med* 2008;205:295-303.
5. Wackerhage H, Del Re DP, Judson RN, Sudol M, Sadoshima J. The Hippo signaling transduction network in skeletal and cardiac muscle. *Sci Signal* 2014;7:re4.
6. Yu FX, Zhao B, Guan KL. Hippo pathway in organ size control, tissue homeostasis, and cancer. *Cell* 2015;163:811-28.
7. Matsuda T, Zhai P, Sciarretta S, et al. NF2 activates Hippo signaling and promotes ischemia/reperfusion injury in the heart. *Circ Res* 2016;119:596-606.
8. Shao D, Zhai P, Del Re DP, et al. A functional interaction between Hippo-YAP signalling and FoxO1 mediates the oxidative stress response. *Nat Commun* 2014;5:3315.
9. Lin Z, von Gise A, Zhou P, et al. Cardiac-specific YAP activation improves cardiac function and survival in an experimental murine myocardial infarction model. *Circ Res* 2014;115:354-63.
10. Leach JP, Heallen T, Zhang M, et al. Hippo pathway deficiency reverses systolic heart failure after infarction. *Nature* 2017;550:260-4.
11. Del Re DP, Yang Y, Nakano N, et al. Yes-associated protein isoform 1 (Yap1) promotes cardiomyocyte survival and growth to protect against myocardial ischemic injury. *J Biol Chem* 2013;288:3977-88.
12. Xin M, Kim Y, Sutherland LB, et al. Hippo pathway effector Yap promotes cardiac regeneration. *Proc Natl Acad Sci U S A* 2013;110:13839-44.
13. Zhang N, Bai H, David KK, et al. The Merlin/NF2 tumor suppressor functions through the YAP oncoprotein to regulate tissue homeostasis in mammals. *Dev Cell* 2010;19:27-38.
14. Acharya A, Baek ST, Banfi S, Eskociak B, Tallquist MD. Efficient inducible Cre-mediated recombination in Tcf21 cell lineages in the heart and kidney. *Genesis* 2011;49:870-7.
15. Kim JE, Nakashima K, de Crombrughe B. Transgenic mice expressing a ligand-inducible cre recombinase in osteoblasts and odontoblasts: a new tool to examine physiology and disease of postnatal bone and tooth. *Am J Pathol* 2004;165:1875-82.
16. Molkenin JD, Bugg D, Ghearing N, et al. Fibroblast-specific genetic manipulation of p38 mitogen-activated protein kinase in vivo reveals its central regulatory role in fibrosis. *Circulation* 2017;136:549-61.
17. Jonsson MKB, Hartman RJG, Ackers-Johnson M, et al. A transcriptomic and epigenomic comparison of fetal and adult human cardiac fibroblasts reveals novel key transcription factors in adult cardiac fibroblasts. *J Am Coll Cardiol Basic Trans Science* 2016;1:590-602.
18. Small EM, Thatcher JE, Sutherland LB, et al. Myocardin-related transcription factor-a controls myofibroblast activation and fibrosis in response to myocardial infarction. *Circ Res* 2010;107:294-304.
19. Yu OM, Miyamoto S, Brown JH. Myocardin-related transcription factor A and yes-associated protein exert dual control in G protein-coupled receptor- and RhoA-mediated transcriptional regulation and cell proliferation. *Mol Cell Biol* 2015;36:39-49.
20. Haak AJ, Tsou PS, Amin MA, et al. Targeting the myofibroblast genetic switch: inhibitors of myocardin-related transcription factor/serum response factor-regulated gene transcription prevent fibrosis in a murine model of skin injury. *J Pharmacol Exp Ther* 2014;349:480-6.
21. Abe H, Takeda N, Isagawa T, et al. Macrophage hypoxia signaling regulates cardiac fibrosis via Oncostatin M. *Nat Commun* 2019;10:2824.
22. Liu F, Lagares D, Choi KM, et al. Mechano-signaling through YAP and TAZ drives fibroblast activation and fibrosis. *Am J Physiol Lung Cell Mol Physiol* 2015;308:L344-57.
23. Mannaerts I, Leite SB, Verhulst S, et al. The Hippo pathway effector YAP controls mouse hepatic stellate cell activation. *J Hepatol* 2015;63:679-88.
24. Liang M, Yu M, Xia R, et al. Yap/Taz deletion in Gli(+) cell-derived myofibroblasts attenuates fibrosis. *J Am Soc Nephrol* 2017;28:3278-90.
25. Xiao Y, Hill MC, Li L, et al. Hippo pathway deletion in adult resting cardiac fibroblasts initiates a cell state transition with spontaneous and self-sustaining fibrosis. *Genes Dev* 2019;33:1491-505.
26. Khalil H, Kanisicak O, Prasad V, et al. Fibroblast-specific TGF-beta-Smad2/3 signaling underlies cardiac fibrosis. *J Clin Invest* 2017;127:3770-83.
27. Davis J, Burr AR, Davis GF, Birnbaumer L, Molkenin JD. A TRPC6-dependent pathway for myofibroblast transdifferentiation and wound healing in vivo. *Dev Cell* 2012;23:705-15.
28. Davis J, Salomonis N, Ghearing N, et al. MBNL1-mediated regulation of differentiation RNAs promotes myofibroblast transformation and the fibrotic response. *Nat Commun* 2015;6:10084.
29. Wang DZ, Li S, Hockemeyer D, et al. Potentiation of serum response factor activity by a family of myocardin-related transcription factors. *Proc Natl Acad Sci U S A* 2002;99:14855-60.
30. Miralles F, Posern G, Zaromytidou AI, Treisman R. Actin dynamics control SRF activity by regulation of its coactivator MAL. *Cell* 2003;113:329-42.
31. Zhao X, Ding EY, Yu OM, et al. Induction of the matricellular protein CCN1 through RhoA and MRTF-A contributes to ischemic cardioprotection. *J Molec Cellular Cardiol* 2014;75:152-61.
32. Foster CT, Gualdrini F, Treisman R. Mutual dependence of the MRTF-SRF and YAP-TEAD pathways in cancer-associated fibroblasts is indirect and mediated by cytoskeletal dynamics. *Genes Dev* 2017;31:2361-75.
33. Liao XH, Wang N, Liu QX, et al. Myocardin-related transcription factor-A induces cardiomyocyte hypertrophy. *IUBMB Life* 2011;63:54-61.
34. Hiemer SE, Szymaniak AD, Varelas X. The transcriptional regulators TAZ and YAP direct transforming growth factor beta-induced tumorigenic phenotypes in breast cancer cells. *J Biol Chem* 2014;289:13461-74.
35. Lauriol J, Keith K, Jaffre F, et al. RhoA signaling in cardiomyocytes protects against stress-induced heart failure but facilitates cardiac fibrosis. *Sci Signal* 2014;7:ra100.
36. Lindsey ML, Bolli R, Canty JM, et al. Guidelines for experimental models of myocardial ischemia and infarction. *Am J Physiol Heart Circ Physiol* 2018;314(4):H812-38.
37. Murphy E, Steenbergen C. Gender-based differences in mechanisms of protection in myocardial ischemia-reperfusion injury. *Cardiovasc Res* 2007;75:478-86.

**KEY WORDS** cardiac fibrosis, heart failure, Hippo signaling, myocardial infarction, YAP

**APPENDIX** For supplemental methods, tables, and figures, please see the online version of this paper.